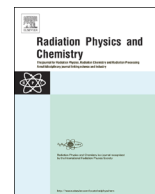




ELSEVIER

Contents lists available at ScienceDirect

## Radiation Physics and Chemistry

journal homepage: [www.elsevier.com/locate/radphyschem](http://www.elsevier.com/locate/radphyschem)

## Nanocomposites of irradiated polypropylene with clay are degradable?



L.G.H. Komatsu, W.L. Oliani, A.B. Lugao, D.F. Parra\*

Nuclear and Energy Research Institute, IPEN-CNEN/SP, Av. Prof. Lineu Prestes, 2242 Cidade Universitária, CEP 05508-000 São Paulo – SP, Brazil

## HIGHLIGHTS

- Nanocomposites of PP were aged under environmental and thermal conditions.
- Barrier effect of clay platelets was verified on the nanocomposites.
- Nanocomposites showed more cracks and surface porosity after environmental ageing.
- Carbonyl indexes were lower in nanocomposites than in the irradiated PP.

## ARTICLE INFO

## Article history:

Received 1 December 2014

Received in revised form

25 May 2015

Accepted 2 June 2015

Available online 17 June 2015

## Keywords:

Polypropylene

Montmorillonite

Nanocomposite

Irradiation process

## ABSTRACT

In nowadays, polypropylene (PP) based nanocomposites containing organically modified montmorillonite (MMT), have gained great attention in the automobilistic industries, construction, paints, packaging, plastic components of the telecommunication industries. The HMSPP (high melt strength polypropylene) is a polypropylene modified by irradiation process, under acetylene atmosphere, in which irradiation occurs in  $^{60}\text{Co}$  gamma source. However, when those materials are submitted to environmental ageing nanocomposites demonstrated high decomposition level after 1 year. This fact can be due to presence the metallic ions present in the montmorillonite. The HMS-PP and the Cloisite 20A (MMT) were mixed in twin-screw extruder using maleic anhydride as compatibilizer. In this work two formulations of nanocomposites at 0.1 and 5 wt% of clay were submitted to the environmental and thermal ageing to analyze the effects of degradation on the HMSPP nanocomposites. The evaluation of thermal properties was analyzed by Differential Scanning Calorimetry (DSC) and the chemical alterations were investigated by Carbonyl Index (CI), through Fourier Transformed Infrared (FTIR) technique. The basal distance was measured by X-ray diffraction (DRX) and the clay elements were analyzed by X-ray Fluorescence (WDXRF). The aim of this work was to understand the effects of degradation of the HMS-PP/clay nanocomposites.

© 2015 Elsevier Ltd. All rights reserved.

## 1. Introduction

Use of radiation to modify the molecular structure and enhancing strain hardening of PP melt, allows to use in areas such as foaming, thermoforming, extrusion coating and blow molding (Gotsis et al., 2004). The high melt strength of a polymer is either due to long chain branching or high molecular weight (Graebing, 2002).

The chemical modification initiated by radicals and the grafting reactions of different monomers on to polypropylene (iPP) in the solid state with the use of grafting at low reaction temperatures,  $\gamma$ , or electron-ray scattering or special peroxides were studied by Rätzsch et al. (2002). Polypropylene irradiated with electrons or gamma-rays undergoes chain scission, and the macroradicals

generated form branched macromolecules. Information on the irradiation modification of the molecular structure of PP is still limited in the literature, especially with respect to the controlled generation of long-chain-branches (LCB) (Auhl et al., 2012).

The research group of Prof. Busfield and Appleby (1986), reported the effects of crosslink enhancement by the presence of acetylene during gamma irradiation, on the physical and mechanical properties of polypropylene.

Jones and Ward (1996), in experimental analysis of the radiation-induced crosslinking of a linear low density polyethylene (LLDPE) film, measured gel fractions as a function of dose, both in vacuum and in presence of acetylene gas and in fact crosslinking was accelerated by the use of acetylene.

Grafting of long-chain-branches on PP backbone using acetylene as a crosslink promoter was developed for production of branched PP under gamma radiation process and was reported (Lugao et al., 2007; Oliani et al., 2012).

\* Corresponding author.

E-mail address: [dfparra@ipen.br](mailto:dfparra@ipen.br) (D.F. Parra).

Concerning polymer nanocomposites (PNCs) area, it has been attracted substantial scientific interest and developments over the last two decades with a huge market opportunity especially for the automotives and packaging industries (Okamoto, 2006). Composites of HMSPP with montmorillonite have few references in the literature (Bhattacharya et al., 2009), mainly considering the aspect of stability under weather conditions or thermal exposition. Polymers exposed to outdoors can degrade through the action of several agents, including solar ultraviolet (UV) radiation; water; pollutants (in gaseous form or, more potently, as acid-rain); elevated temperature. In a majority of cases, the main cause of property deterioration is photo-oxidation, which is initiated by UV irradiation and, as a consequence, much laboratory photo-ageing testing was conducted to determine the weatherability of polymers and to test the effectiveness of stabilizers to improve their weather resistance (White, 2006; Singh and Sharma, 2008; Rivaton et al., 2005; Attwood et al., 2006; Oliani et al., 2010).

Polypropylene undergoes predominantly chain scission under all processing conditions giving rise to pronounced reduction in the molar mass and melt viscosity of the polymer (Al-Malaika, 2003) other than melting temperature and normally increasing of crystallinity.

Abiotic peroxidation of the polyolefins, gives rise to some vicinal hydroperoxides and this process is particularly favored in the poly- $\alpha$ -olefins, such as polypropylene due to the susceptibility of the tertiary carbon atom to hydrogen abstraction via a hydrogen-bonded intermediate. A major proportion of the peroxide product are hydrogen-bonded vicinal hydroperoxides that break down to small biodegradable molecules such as carboxylic acids, alcohols and ketones (Wiles and Scott, 2006; Morlat et al., 2004).

One of the main aspects in the development of polymer nanocomposites is the matrix degradation. In a work of Ramos Filho et al., (2005) a polycationic bentonite clay was added to isotactic polypropylene (iPP). The compounds were prepared by melt intercalation using a twin extruder, similar to work of Komatsu et al., (2014a,b). Under 110 °C for up to 165 h, the degradation of the composites was more intense than the unfilled polymer and this may be due to the presence of acidic sites on the clay surface that act as a catalyst to the polymer oxidation, and/or due to salt decomposition, initiating the free radical degradation of iPP.

The aim of present work was to understand the degradation effects of HMSPP/Clay nanocomposites, under thermal and environmental conditions, considering the new morphology created by the irradiation in acetylene, and the presence of clay.

## 2. Experimental

### 2.1. 1 Materials and methods

The iPP pellets were manufactured by Braskem and compatibilizer agent, propylene maleic anhydride graft copolymer (PP-g-MA) was supplied by Addivant (Polybond 3200). The clay filler was Cloisite 20A by Southern Clay Products montmorillonite clay quaternary ammonium salt-modified (95 Meq/100 g). The iPP was placed in plastic bags with acetylene that were irradiated in  $^{60}\text{Co}$  gamma source at dose of 12.5 kGy in order to obtain the HMSPP. The iPP utilized in this work has no nucleating agent or stabilizing in it formulation. Two different formulations containing the clay were prepared and are represented in Table 1. The samples were prepared in molten state using a twin-screw extruder (Thermo Haake Polymer Laboratory) to incorporate the clay in the polypropylene. The operated temperatures were 170–200 °C and speed ranging from 30 to 60 rpm. The dumbbell samples for testing were obtained from thermal molding pressure (80 bar and 190 °C), for type IV dimensions according to ASTM D638-03. After molding,

**Table 1**  
Content of clay and compatibilizer used in the samples.

Samples	Matrix	PP-g-MA (%)	Cloisite 20A (%)
H1	HMSPP	–	–
NC1	HMSPP	3	0.1
NC2	HMSPP	3	5

the dumbbell samples were mounted in appropriated device for environmental and thermal ageing, as illustrated in Fig. 1.

#### 2.1.1. Differential scanning calorimetry

Thermal properties of specimens were analyzed using a differential scanning calorimeter (DSC) 822, Mettler Toledo. The thermal behavior of the films was obtained by: heating from 25 to 280 °C at a heating rate of 10 °C min<sup>-1</sup> under nitrogen atmosphere, according to ASTM D 3418-08. The crystallinity was calculated according to the equation:

$$x_c = p \times \frac{\Delta H_f \times 100}{\Delta H_0} \quad (1)$$

where:  $\Delta H_f$  is melting enthalpy of the sample,  $\Delta H_0$  is melting enthalpy of the 100% crystalline PP which is assumed to be 209 kJ kg<sup>-1</sup> (Brandrup et al., 1999; Mark, 2007).

#### 2.1.2. Scanning electron microscopy

Scanning electron microscopy was done using an EDAX PHILIPS XL 30. In this study, a thin coat of gold was sputter-coated onto the samples.

#### 2.1.3. Fourier transformed infrared spectroscopy

Infrared spectroscopy was performed at Thermo Scientific (Nicolet 6700) with ATR accessory Smart Orbit Diamond, in the range from 400 to 4000 cm<sup>-1</sup>.

#### 2.1.4. X-ray diffraction

X-ray diffraction measurements were carried out in the reflection mode on a Rigaku diffractometer Mini Flex II (Tokyo, Japan) operated at 30 kV voltage and a current of 15 mA with CuK $\alpha$  radiation ( $\lambda = 1,541841 \text{ \AA}$ ).

#### 2.1.5. X-ray fluorescence

The sample of Cloisite 20A was placed in a crucible and then placed in a muffle furnace at 900 °C to eliminate volatile components. The pastille was made pressing it under one layer of boric acid. The analysis was operated in spectrometer equipment Rigaku Fluorescence X-ray, model RIX.

## 3. Results and discussion

To understand the effects of environmental and thermal ageing in the polypropylene nanocomposites, the X-ray fluorescence technique was utilized to evaluate the clay composition, as presented in Table 2.

In Table 2 is observed presence of pro-oxidant elements as: Al, Fe and Mg. In the literature is reported that low quantities of these elements acts as oxidants of polymers by redox reactions with hydroperoxides (Morlat-Therias et al., 2005).

Results of FT-IR are presented in Fig. 2 while carbonyl group was identified at 1720 cm<sup>-1</sup> and the peak of 1048 cm<sup>-1</sup> is attributed to Si–O–Si bonds.

In the Fig. 3, are represented the carbonyl indexes (CI), calculated utilizing the carboxylic acid band (carbonyl stretching) around 1720 cm<sup>-1</sup>, and the band 2720 cm<sup>-1</sup>, as reference. This

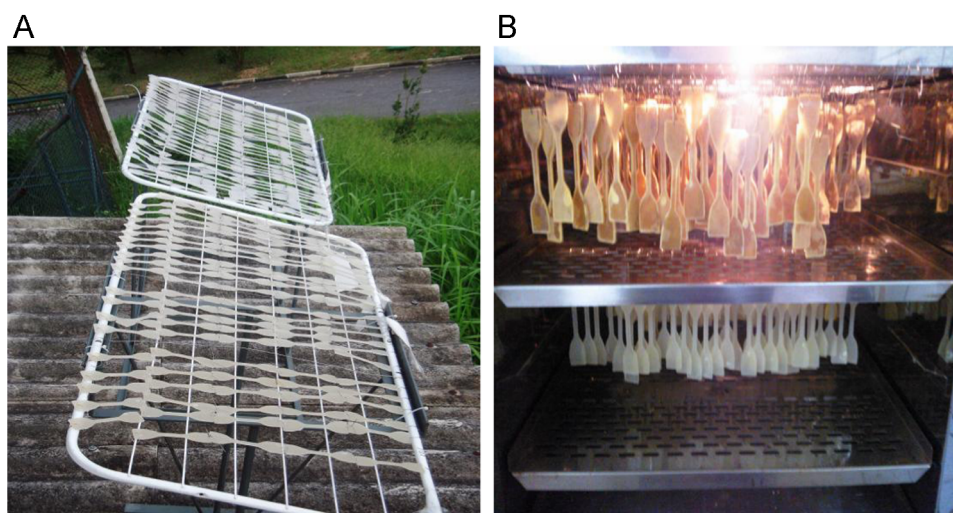


**Fig. 1.** (A) Device with dumbbell samples for environmental ageing exposed outside at the IPEN/CQMA, and (B) nanocomposite samples in air circulation stove at the temperature of 110 °C.

**Table 2**  
Chemical composition of montmorillonite clay.

Components	Content (%)
Loss on ignition	34.0 ± 0.3
SiO <sub>2</sub>	43.0 ± 0.4
Al <sub>2</sub> O <sub>3</sub>	16.8 ± 0.2
Fe <sub>2</sub> O <sub>3</sub>	3.6 ± 0.2
MgO	2.0 ± 0.1
Na <sub>2</sub> O	0.20 ± 0.02
K <sub>2</sub> O	0.023 ± 0.002
Cl	0.19 ± 0.01
CaO	0.11 ± 0.01
TiO <sub>2</sub>	0.09 ± 0.01

functional group is produced by alkyl radicals and oxygen reactions. To a certain extent, an alkoxide radical takes an electron from a carbon–carbon bond. This event transforms the oxidized group into carbonyl and the polymeric chain undergoes a mechanism called  $\beta$ -scission (Silvano et al., 2013). Fig. 3 represents the carbonyl index calculated for environmentally aged samples (A) and thermal aged samples (B). The thermal degradation was intensified drastically in 21 days and compared with environmental condition at one month, the metal ions of the clay act as

oxidants catalyzed by temperature.

The Fig. 3(A), the metallic ions present in the clay composites promote the oxidation of the surfaces in the early periods of exposition (up to 4 month). In this photo-oxidation phenomenon the competitive mechanism is the “screening effect”, where the clay lamellae acts as a filter to UV radiation, so in this case of the exfoliated clay can be more efficient as observed in the 0.1% clay composite. Above to 4 months the H1 that has no oxidation protection shows the CI continuously intensified.

In Fig. 3(B), the thermal degradation is intensified in the nanocomposite, while the sample H1 is almost stable, with minor oxidation detected similar to 1 month of Fig. 3(A). This fact reveals that thermal oxidation of the surfaces is strongly intensified in presence of the clay.

Barrier effect is considered when assumed the diffusion of oxygen to the bulk of the composite. According to Bartolucci et al. (2013), the clay layers act as barrier to the oxygen diffusion into the nanocomposite. So this effect can be evaluated in the interior of the sample by observing the crystallinity and melting temperature of the crystallites. In Tables 3, 4 and 5 are shown the effects of ageing assays on the crystallinity and melting temperature of the samples. In the sample NC2 the effect barrier was observed at 3 and 6 months, when the values of  $T_{m1}$  and  $X_c$  are

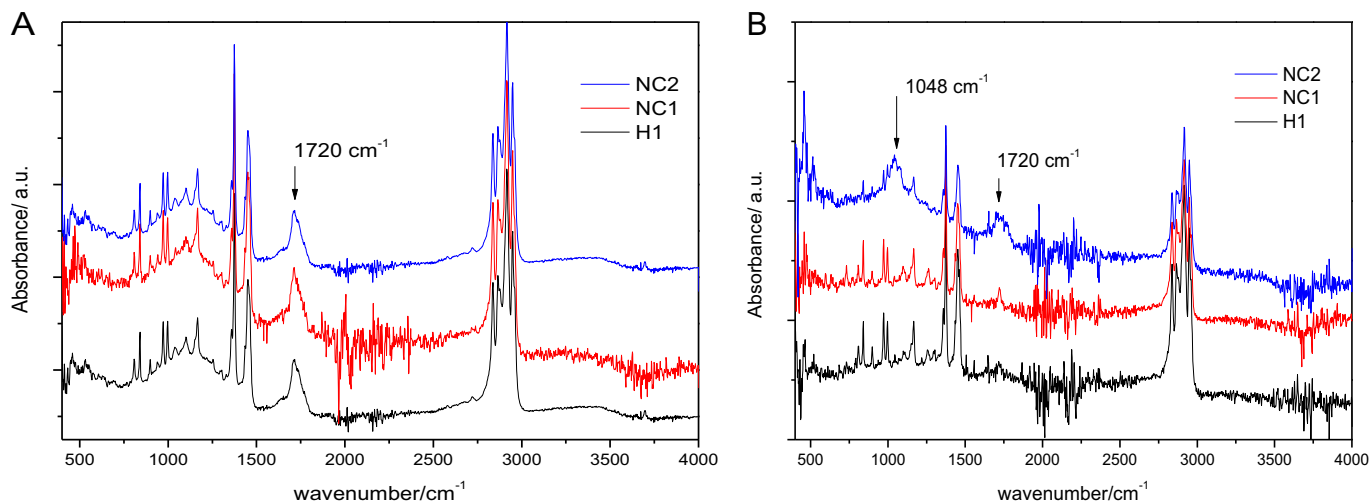


**Fig. 2.** FT-IR of environmental aged samples after 6 months (A), and thermal aged samples after 21 days in stove (B).

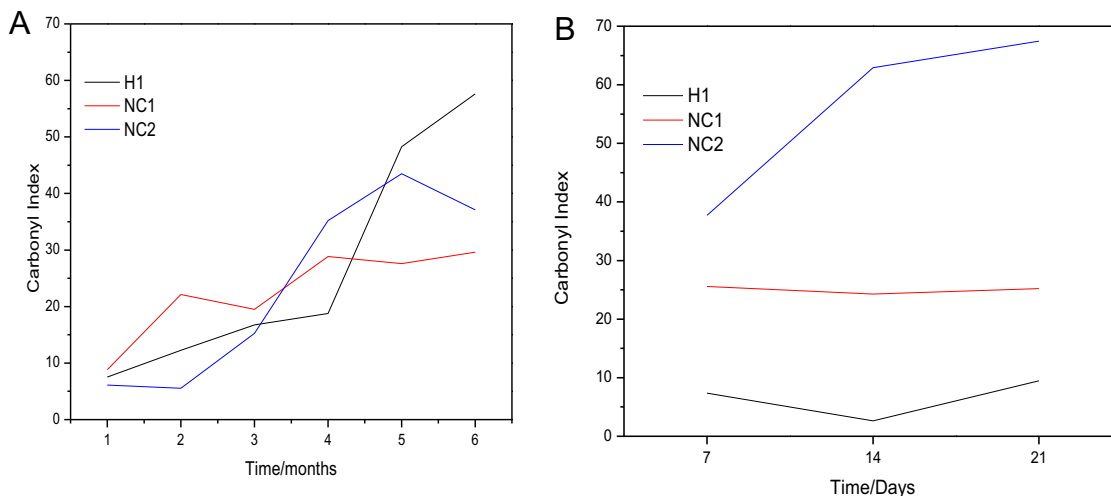


Fig. 3. Carbonyl Index of samples: (A) environmental aged and (B) thermal aged.

Table 3

Crystallization temperature  $T_c$ , melting temperature  $T_{m1}$  and crystallinity  $X_c$  of sample H1.

	Environment/months				Thermal/days			
	Zero	3	6	12	7	14	21	28
Time	Zero	3	6	12	7	14	21	28
$T_{m1}$ (°C)	165.7	158.7	156.9	151.6	169	168.4	167.5	165.5
$X_c$ (%)	41.1	43.1	45.5	45.8	49.9	46.9	49.4	52.0

Table 4

Crystallization temperature  $T_c$ , melting temperature  $T_{m1}$  and crystallinity  $X_c$  of sample NC1.

	Environment/months				Thermal/days			
	Zero	3	6	12	7	14	21	28
Time	Zero	3	6	12	7	14	21	28
$T_{m1}$ (°C)	167.6	152.3	148.6	158.0	178.0	178.1	163.6	164.6
$X_c$ (%)	44.1	46.6	47.5	48.9	45.4	43.6	56.0	54.9

Table 5

Crystallization temperature  $T_c$ , melting temperature  $T_{m1}$  and crystallinity  $X_c$  of sample NC2.

	Environment/months				Thermal/days			
	Zero	3	6	12	7	14	21	28
Time	Zero	3	6	12	7	14	21	28
$T_{m1}$ (°C)	167.7	178.03	159.2	143.0	167.7	164.9	153.4	153.5
$X_c$ (%)	37.9	42.8	42.9	52.6	48.1	41.4	54.1	55.0

almost constant. After this period of time the oxygen penetrates

and accelerates the photo-oxidation condition on the nanocomposite NC2. The barrier effect was not observed in NC1 considering these properties.

During environmental ageing the sample H1 suffers chain scission due UV components of the sun light of environmental exposition, with decrease of  $T_{m1}$  with, in consequence, increase in crystallinity. During thermal ageing also is observed increase of crystallinity.

In the environmental ageing, the chain scission occurs on the NC1 and the crystallinity tends to be higher after 6 months as for chemicrystallization effect, as reported by Mouzakis et al., (2006). The amount of clay is not enough to prevent the chemicrystallization at long time.

SEM images of the samples NC2 after 12 months of environmental ageing (Fig. 4A) and after 28 days of thermal ageing (Fig. 4B) present a cracked surfaces.

Intense cracks are observed on the surfaces as for effect of chemicrystallization. This effect causes the contraction of the layers with formation of cracks, intensely and deeper. In the sample environmentally aged the surface showed, others than cracks, porosity, a visual effect of degradation by of metallic ions present in the MMT, as previously observed by Morlat-Therias et al., (2005).

In Table 6 are presented the results of DRX analysis and the occurrence of intercalation of the clay in the polymer matrix, verified by increase of lamellar distance of the clay in the nanocomposite, in the NC2 while in NC1 has evidence of exfoliation.

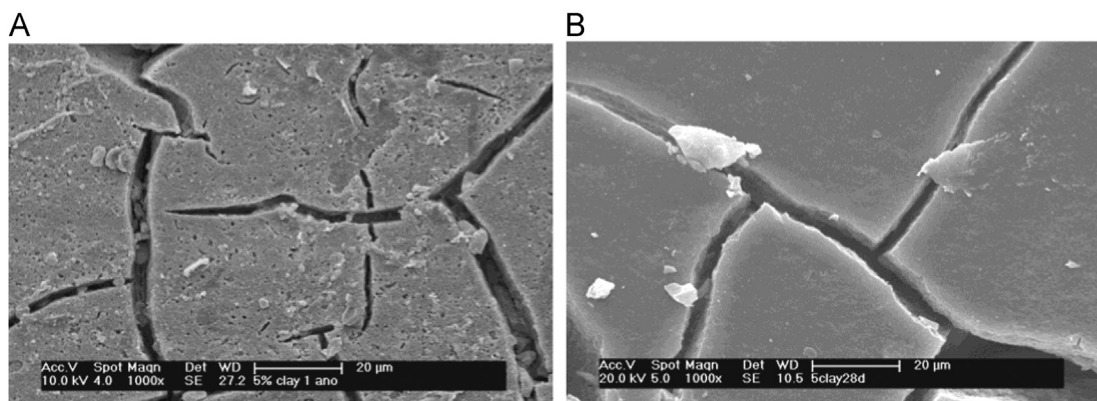


Fig. 4. SEM of environmentally aged sample after 12 months (A), thermal aged sample after 28 days (B).

**Table 6**  
Interlamellar distances of MMT in the nanocomposite.

Samples	$d_{001}$ (Å)
Cloisite 20A	24.4
NC1	–
NC2	30.8

#### 4. Conclusions

The nanocomposites were obtained with intercalation of the polymer in the lamellar structure of the clay.

The nanocomposites were aged in two different conditions: thermal and environmental. Compared to the H1, iPP modified by irradiation process, the nanocomposites environmental exposition, have the metallic ions that promote the surface oxidation in the early periods of exposition (up to 4 month). Because the competitive mechanism of the “screening effect”, where the clay lamellae acts as a filter to UV radiation, the exfoliated clay can be more efficient as observed in the 0.1% clay composite. Above 4 months the H1 has no oxidation protection and the CI is continuously intensified.

In the sample NC2 the effect barrier was observed at 3 and 6 months, when the values of  $T_{m1}$  and  $X_c$  are almost constant. After this period of time the oxygen penetrates and accelerates the photo-oxidation on the nanocomposite NC2. The barrier effect was not an evidence in NC1 considering these properties.

In consequence of thermal degradation the nanocomposite were drastically modified. The sample H1 performed better thermal stability than the nanocomposites for the surfaces oxidation (CI) with formation of cracks (new surfaces) in the early periods of ageing.

#### Acknowledgments

The authors thank CAPES, Brazil; Fapesp, Brazil (2014/26393-1) and CNPQ, Brazil for grants in SWB program, Centre of Science and Technology of Materials – CCTM/IPEN, for microscopy analysis (SEM), the technicians Mr. Eleosmar Gasparin and Nelson R. Bueno, for technical support, Southern Clays, Addivant and Companhia Brasileira de Esterilização (CBE) for irradiating the samples.

#### References

- Al-Malaika, S., 2003. Oxidative degradation and stabilisation of polymers. *Int. Mater. Rev.* 48 (3), 165–185.
- ASTM D 638–03 – Standard Test Method for Tensile Properties of Plastics.
- ASTM D 3418–2008—Standard test method for transition temperatures and enthalpies of fusion and crystallization of polymers by differential scanning calorimetry.
- Attwood, J., Philip, M., Hulme, A., Williams, g, Shipton, P., 2006. The effects of ageing

- by ultraviolet degradation of recycled polyolefin blends. *Polym. Degrad. Stab.* 91, 3407–3415.
- Auhl, D., Stadler, F.J., Münstedt, H., 2012. Comparison of molecular structure and rheological properties of electron beam and gamma irradiated polypropylene. *Macromolecules* 45, 2057–2065.
- Bartolucci, S.F., Supan, K.E., Wiggins, J.S., LaBeaud, L., Warrender, J.M., 2013. Thermal stability of polypropylene-clay nanocomposites subjected to laser pulse heating. *Polym. Degrad. Stab.* 98, 2497–2502.
- Bhattacharya, S., Gupta, R.K., Jollands, M., Bhattacharya, S.N., 2009. Foaming behavior of high-melt strength polypropylene/clay nanocomposites. *Polym. Eng. Sci.* 10, 2070–2084.
- Brandrup, J., Immergut, E.H., Grulke, E.A., 1999. *Polymer Handbook*, fourth ed. Vol 1. Wiley Interscience, New York.
- Busfield, W.K., Appleby, R.W., 1986. Crosslink enhancement in polypropylene film by gamma irradiation in the presence of acetylene. *Br. Polym. J.* 18, 340–344.
- Gotsis, A., Zeevenhoven, B., Hogt, A., 2004. The effect of long chain branching on the processability of polypropylene in thermoforming. *Polym. Eng. Sci.* 44, 973–982.
- Graebbling, D., 2002. Synthesis of branched polypropylene by a reactive extrusion process. *Macromolecules* 35, 4602–4610.
- Jones, R.A., Ward, I.M., 1996. Reactions of amorphous PE radical-pairs in vacuo and in acetylene a comparison of gel fraction data with Flory-Stockmayer and atomistic modelling analyses. *Polymer* 37 (16), 3643–3656.
- Komatsu, L.G.H., Oliani, W.L., Lugao, A.B., Parra, D.F., 2014a. Environmental ageing of irradiated polypropylene/montmorillonite nanocomposites obtained in molten state. *Radiat. Phys. Chem.* 97, 233–238.
- Komatsu, L.G.H., Oliani, W.L., Ferreto, H.F.R., Lugao, A.B., Parra, D.F., 2014b. Effects of environmental ageing on HMS-polypropylene/Cloisite nanocomposites. *AIP Conf. Proc.* 1593, 257. <http://dx.doi.org/10.1063/1.4873776>.
- Lugao, A.B., Otaguro, H., Parra, D.F., Yoshiga, A.Y., Lima, L.F.C.P., Artel, B.W.H., Liberman, S., 2007. Review on the production process and uses of controlled rheology polypropylene-gamma radiation versus electron beam processing. *Radiat. Phys. Chem.* 76, 1688–1690.
- Mark, J.E., 2007. Chapter 39 – crystallization kinetics of polymer, *Physical Properties of Polymers Handbook*. Springer, Cincinnati-USA, p. 639.
- Morlat, S., Mailhot, B., Gonzalez, D., Gardette, J.L., 2004. Photooxidation of polypropylene/montmorillonite nanocomposites. 1. Influence of nanoclay and compatibilizing agent. *Chem. Mater.* 16, 377–383.
- Morlat-Therias, S., Mailhot, B., Gonzalez, D., Gardette, J.L., 2005. Photo-oxidation of polypropylene/montmorillonite nanocomposites. 2. Interactions with anti-oxidants. *Chem. Mater.* 17, 1072–1078.
- Mouzakis, D.E., Kandilioti, G., Elenis, A., Gregoriou, V.G., 2006. Ultraviolet radiation induced cold chemi-crystallization in syndiotactic polypropylene clay-nanocomposites. *J. Macromol. Sci. A* 43, 259–267.
- Okamoto, M., 2006. Recent advances in polymer/layered Silicate nanocomposites: in overview from science to technology. *Mater. Sci. Technol.* 22 (7), 756–779.
- Oliani, W.L., Parra, D.F., Lima, L.F.C.P., Lugao, A.B., 2012. Morphological characterization of branched PP under stretching. *Polym. Bull.* 68, 2121–2130.
- Oliani, W.L., Parra, D.F., Lugao, A.B., 2010. UV stability of HMSPP (high melt strength polypropylene) obtained by radiation process. *Radiat. Phys. Chem.* 79, 383–387.
- Ramos Filho, F., Melo, T.J.A., Rabello, M.S., Silva, S.M.L., 2005. Thermal stability of nanocomposites based on polypropylene and bentonite. *Polym. Degrad. Stab.* 89, 383–392.
- Rätzsch, M., Arnold, M., Borsig, E., Bucka, H., Reichelt, N., 2002. Radical reactions on polypropylene in the solid state. *Prog. Polym. Sci.* 27, 1195–1282.
- Rivaton, A., Gardette, J.L., Mailhot, B., Therias, S.M., 2005. Basic aspects of polymer degradation. *Macromol. Symp.* 225, 129–146.
- Silvano, J.R., Rodrigues, S.A., Marini, J., Bretas, R.E.S., Canevarolo, S.V., Carvalho, B.M., Pinheiro, L.A., 2013. Effect of reprocessing and clay concentration on the degradation of polypropylene/montmorillonite nanocomposites during twin screw extrusion. *Polym. Degrad. Stab.* 98, 801–808.
- Singh, B., Sharma, N., 2008. Mechanistic implications of plastic degradation. *Polym. Degrad. Stab.* 93, 561–584.
- Wiles, D.M., Scott, G., 2006. Polyolefins with controlled environmental degradability. *Polym. Degrad. Stab.* 91, 1581–1592.
- White, J.R., 2006. Polymer ageing: physics, chemistry or Engineering? Time to reflect. *C. R. Chim.* 9, 1396–1408.